Microstructures of the Zanskar Shear Zone

Soumyajit Mukherjee
Department of Earth Sciences
Indian Institute of Technology Bombay, Mumbai-400 076
Email: soumyajitm@gmail.com

Abstract

Thin-sections studies of the rocks of the Zanskar Shear Zone led to document a top-to-SW ductile shearing; a top-to-NE shearing and finally a top-to-NE (down) shearing. Shape asymmetry and cleavage orientations of mineral fish reliably give the latter two shear senses. Although some of the fish reveal different phases of shearing, their specific orientations indicates simple shear. Type-1 flanking microstructures indicate the earliest top-to-SW shear. Boudins denote extension along the main foliation. Intrafolial folds demonstrate a top-to-NE shearing. A top-to-SW brittle shear is displayed by asymmetric trapezoid-shaped minerals. The brittle planes cut across rigid minerals. As in other shear zones, micas are found to be most susceptible to deformation.

Introduction

The Zanskar Shear Zone (ZSZ), the northern boundary of the Higher Himalaya in Kashmir, comprises mainly of mylonitized gneisses, leucogranites and migmatites (Fig. 1) where the grade of metamorphism varies from lower greenschist to upper amphibolite facies (Herren, 1987). Note that in Fig. 1, the term 'High Himalaya' of Searle *et al.* (1988) is replaced by 'Higher Himalayan Shear Zone'. The granitic rocks of the area belong to Miocene Period (reviews by Godin *et al.,* 2006; and Yin, 2006). Structural geology and tectonics of this shear zone have been discussed in detail and updated by a number of workers, *e.g.* Herren (1987), Patel *et al.* (1993), Steck *et al.* (1993), Dèzes (1999), Dèzes *et al.* (1999), Walker *et al.* (1999) and Mukherjee and Koyi (in press, 1). The ZSZ characterizes a normal way up isograds (see review in Walker *et al.,* 2001). Dèzes *et al.* (1999) estimated the vertical displacement (minimum amount) and the net slip of the ZSZ to be 12 ± 3 km and 35 ± 9 km, respectively. They also deduced the thickness of the shear zone to be 1 km and observed that the leucogranite dykes are sheared parallel to the foliation planes. Walker *et al.* (1999) estimated the 'total slip' (net slip?) to be 40-60 km. Foliation planes dip 20-30^0, the outcrop width of the ZSZ is about 5 km (Walker *et al*., 1999) and the shear zone can be traced along the Himalayan trend for about 80 km (Herren, 1987). Herren (1987) and Walker *et al.* (1999) estimated the throw of the ZSZ to be ~ 15-20 km. Herren (1987) noted a top-to-NE sense of extensional ductile shearing from the ZSZ. Subsequent work by Patel *et al.* (1993) and Dèzes *et al.* (1999) revealed a relict top-to-SW shear sense too. Mukherjee and Koyi (in press, 1) recently documented three phases of ductile deformation in micro-scale on a plane perpendicular to the northeasterly dipping main foliation and parallel to the northeasterly plunging stretching lineation. These three phases are (i) a top-to-SW sense of compressional shearing ('shearing-1'), (ii) subsequent top-to-NE sense of extensional shearing ('shearing-2'), and (iii) a latest top-to-NE (down) sense of extensional ductile shearing ('shearing-3'). Out of these, shearing-1 and 3 were first documented from field by Patel *et al.* (1993) and subsequently by Dèzes (1999) and Dèzes *et al.* (1999). In addition, Mukherjee and Koyi (op. cit.) showed (i) different varieties of micro-boudins parallel to the main foliation indicating a brittle-ductile extension parallel to the foliation, (ii) symmetric duplexes of high-grade minerals not indicative of any

brittle shear sense, (iii) asymmetric duplexes of low-grade minerals indicating a top-to-SW sense of brittle shearing, (iv) northeasterly dipping sharp brittle normal micro-faults, (v) transgranular fractures (or T-fractures) that cut the primary shear planes at high angles, and (v) extensive grain boundary migrations. The angular relations measured under microscope by Mukherjee and Koyi (in press, 1) is summarized in Table-1.
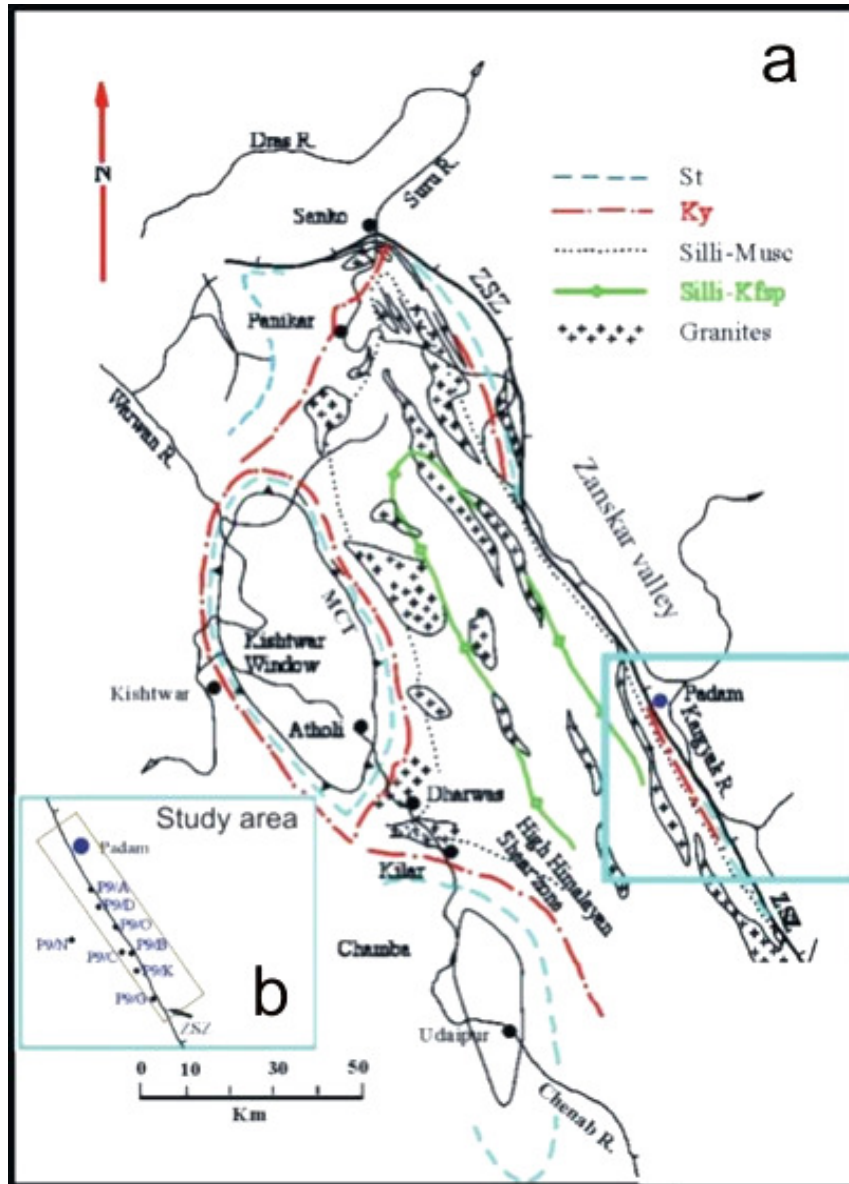
Fig. 1 a: Geological map of the Higher Himalayan Shear Zone in the Zanskar–Chamba–Kulu area, reproduced from Searle *et al.* (1988). Isograds are shown. The studied thin-sections are from rocks within the Zanskar Shear Zone SE to the locality Padam. **b.** Locations of rock samples SE to Padam.

Table-1: Micro-structural data of the ZSZ as compiled from Mukherjee (2007) and Mukherjee and Koyi (in press, 1). Symbols: top-to-NE (down) ductile shearing: 'shearing-3', top-to-NE ductile shearing: 'shearing-2', top-to-SW ductile shearing: 'shearing-1'. All measurements were done on the XZ thin-sections.

Serial Number	Shearing-3:		Shearing-2		Shearing-1
	Angle between S & C planes	Angle between axial trace & C-plane	Angle between axial trace & C plane	Angle between S &C planes	Angle between S &C planes
1-5	47^0	70^0	13 to 21^0	30^0	4 to 8^0
6	Mineral fish with aspect ratios: 2 to 4.8				
7	Mineral fish: angles between long axes & ductile shear plane: 0-32^0				
8	Angle between ductile shear planes of shearing-1 and shearing-3: 25-53^0				
9	Primary shear planes for shearing-1 and -2 coincide				
10	Angles between P- and Y-brittle shear planes vary up to 35^0				
11	The primary brittle shear plane (Y-plane) and the primary shear planes of shearing-1 and -2 coincide				
12	Angle between Y- and secondary synthetic brittle shear R-plane ~ 15^0				
13	Angle between T-fractures and Y-plane: 69-86^0				
14	Angle of V in V-pull-aparts: 10-27^0				
15	Aspect ratios of boudins: 3.3-4.2				

Walker *et al.* (2001) considered the timing of extrusion of the HHSZ in the Zanskar section to be 21.5-19.5 Ma. On the other hand, compiling existing geochronological data, Mukherjee and Koyi (in press, 1) interpreted the top-to-SW sense of shearing in the ZSZ to be a ~22-16 Ma event and as a delayed product of India-Eurasia collision. The extensional ductile shearing was interpreted to be of a shorter span of ~18-16 Ma. During ~18-16 Ma was in fact the span of combined activation of top-to-SW and –NE shearing. Brittle fractures were considered as perturbing events to the southwesterly brittle shearing. Recently channel flow model (Beaumont *et al.,*2001) has evolved as an almost unanimously accepted extrusion mechanism of the HHSZ (see review in Mukherjee, 2005). Mukherjee and Koyi (in press, 1) applied a combined simple shear and channel flow model of extrusion of the HHSZ in the Zanskar section, which is an elaboration of Grujic *et al.'s* (2002) model proposed for the Bhutan Himalaya. This work aims at detail micro-structural studies of the ZSZ rocks.

Microstructures

Mineral fish:

Mineral fish are lozenge-shaped porphyroclasts and single crystals in fine-grained matrices in mylonitized rocks (ten Grotenhuis *et al.* 2002; also see Mukherjee and Pal, 2000). Mineral fish (Figs. 2a-c; 3a-d; 4a-d; 6c; 8d; 12b) are the most common ductile shear sense indicators in the ZSZ in micro-scale. In the studied thin-sections, quartz, muscovites, biotites, feldspars, garnets and staurolites show the characteristic fish shape. Unlike Passchier and Trough's (2005) view that quartz fish are rare in shear zones, they are rather abundant in the ZSZ (Figs. 3c, 4a, 4d, 6c). Where the mineral fish touch the shear planes that bound them, the shear strain is maximum and equidistant from a pair of C-

planes the shear strain is minimum. The C-planes are straight and envelope (or, are tangent to) the mineral fish. These planes are defined by very fine-grained recrystallized minerals. The C-planes seem to be irregularly spaced (Figs. 2d, 3d). Three broad morphologies of mineral fish were observed- (i) sigmoid (Figs. 2a-c, 3a-d, 4a-d); (ii) lenticular (Fig.5c); and (iii) parallelogram (Figs. 7c, 9d). Sigmoid-shaped fabrics show progressive curving near the bounding C-planes. Either these three shapes were defined by single minerals (Figs. 2a-c, 3a, 4b, 4d, 5c, 6c, 8d) or as aggregate of minerals (Figs. 2d, 3b-d, 4a, 4c) that are usually micas. Two senses of ductile shearing are documented from mineral fish- a top-to-NE (Fig. 2a, 2d, 3a-d, 4a, 4c-d, 5d, 6c, 8a, 12b-d) *i.e.* just in the opposite direction to that of the previous top-to-SW sense, and a top-to-NE (down) (Figs. 2a-d, 3a, 4b, 6a, 6c-d, 12b-d). The cleavages of mineral fish are in all cases tilted to the primary shear plane same as that of the fish itself. Thus, the cleavage planes of mineral fish alone can act as reliable shear sense indicators.

Sometimes mineral fish are found to be affected by late brittle shearing (Fig. 6c). Individual minerals, in composites that define the fish, are not indicative of any sense of shearing. These aggregates can be considered as 'decussate texture' (Fig. 6b). For example, the possible shape of a parallelogram grain of mica could be a rectangle such as shown by dashed lines in Fig. 6b, and that grains 'p' and 'q' might have concealed parts of them giving rise to the parallelogram shape. In some cases rigid quartzo-feldspathic minerals are wrapped by incompetent micas that overall defines the fish shape (Figs. 2b, 3d, 4c, 12c). A very peculiar example of a train of muscovite fish nucleated inside a host of muscovite grain (Fig. 11c) was noted. The nucleated muscovite fish display the top-to-SW sense of shearing. In some cases, lenticular fish, presumably products of the prior top-to-SW sense of shearing underwent late brittle top-to-NE shearing (Fig. 11a). In other words, the latter shear sense although most of the times acted ductilely on minerals, at times it also deformed minerals in a brittle manner. Strongly swerved cleavages of mica are found to be in sympathy with the shearing of the clast (*e.g.* Fig. 3a). As in Fig. 2d, the ratio of thicknesses of shear zones formed in micro-scale are 14.3:6.3:1:13. On the other hand in Fig. 3d, the ratio of distances (white lines) between the pair of C-planes to that bounding the clast is 1:15. One of the C-planes could be remarkable straight than the other one. Minerals recrystallized near the C-planes of porphyroclasts define tiny shear zones. The ductile shear planes in parallel arrays could be defined by intense grain size reduction (Fig. 3d).

Many times the same mineral fish are affected by shearing of two phases *i.e.* a top-to-NE and a top-to-NE (down) (Figs. 2a-b). Near their tips, the fish may be kinked as also revealed from their sharply folded cleavage planes (Fig. 8d). In a rare example, the C-planes that bound the top-to-NE shear fabric were found to be non-parallel (Fig. 4a). Extensive migration of boundary of grains from matrix into fish might lead to loss of the fish shape almost beyond recognition. Inclusion of alkali feldspar inside sigmoid mica fish are also noted (Fig. 3a). Such more competent inclusions were found to be undeformed. Extensively recrystallized minerals in the matrix define the S-fabric of Bèrthe *et al.* (1979). Some of the mineral fish possess mouths at their corners (*e.g.* Fig. 4d) probably indicating boudinage from one fish to the adjacent one. Pronounced top-to-NE (down) sense of shearing lowered the local orientation of the mineral fish to the northeasterly dipping main foliation planes. Secondary shearing in some cases led to stair stepping of the fish tails. Pressure solution might be a reason of sigmoidality of some of the fish (*e.g.* Bell and Cuff 1989). A consistent northeast dipping orientation of the primary foliation plane that bound the mineral fish indicate that they certainly were the products of simple shearing and not by pure shear on clasts of significantly different viscosity than the matrix as proposed by Treagus and Lan (2000).
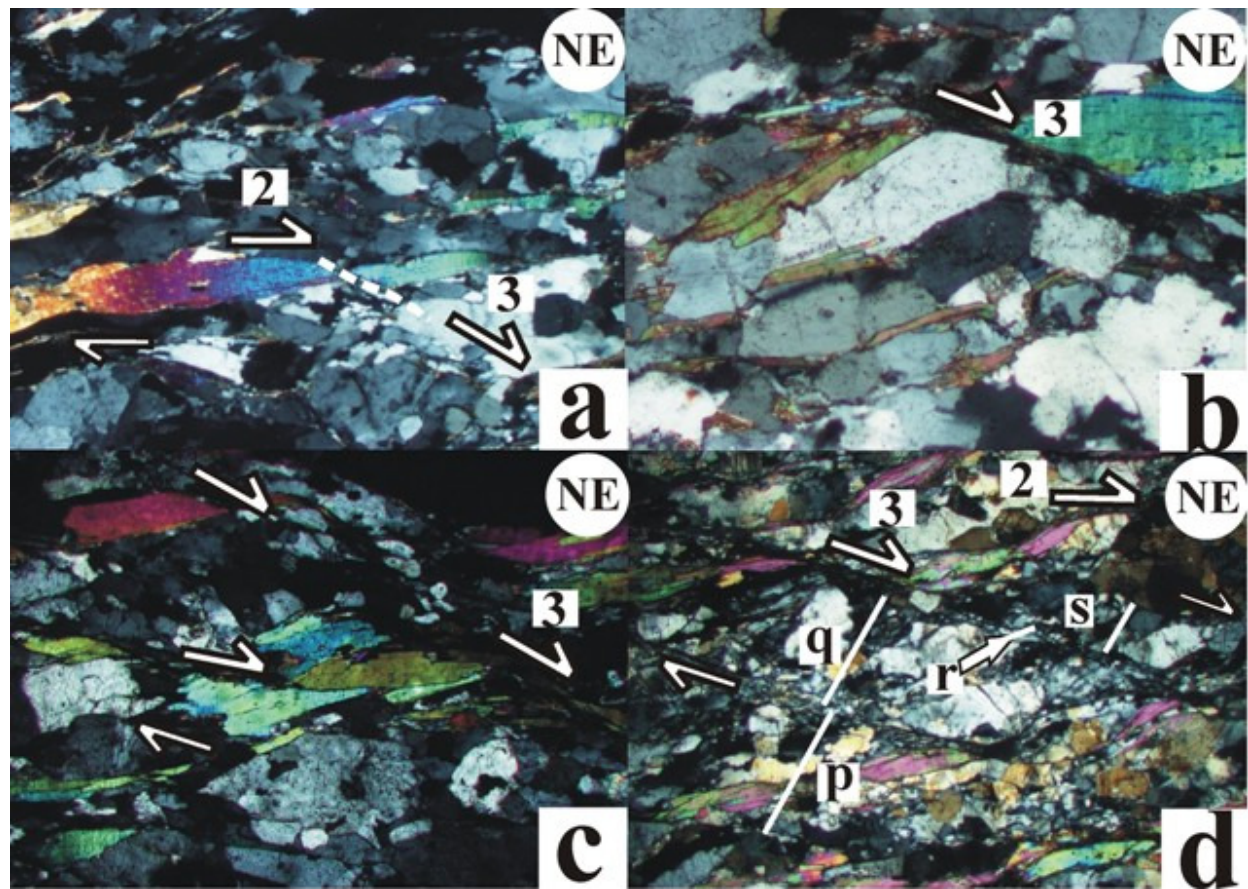
Fig. 2: a. Single sigmoid muscovite fish shows a top-to-NE shear (shearing-2). Top-to-NE (down) shear (shearing-3) brought one of the fish tips at gentler angle to the shear plane of '2'. (Cross-polarized light; photo width: 2 mm.) **b.** A single sigmoid alkali feldspar fish showing a top-to-NE (down) shear (shearing-3). The boundary of this grain is partly occupied by biotites. (Cross-polarized light; Photo width: 1 mm.) **c.** A top-to-NE (down) shear (shearing-3) is indicated by imperfect parallelogram and sigmoid shaped mica fish. (Cross-polarized light; Photo width: 1 mm.) **d.** A top-to-NE (down) shear (shearing-3) is indicated by an aggregate of porphyrclastic nearly sigmoid shaped alkali feldspars. (Cross-polarized light; Photo width: 2 mm.).
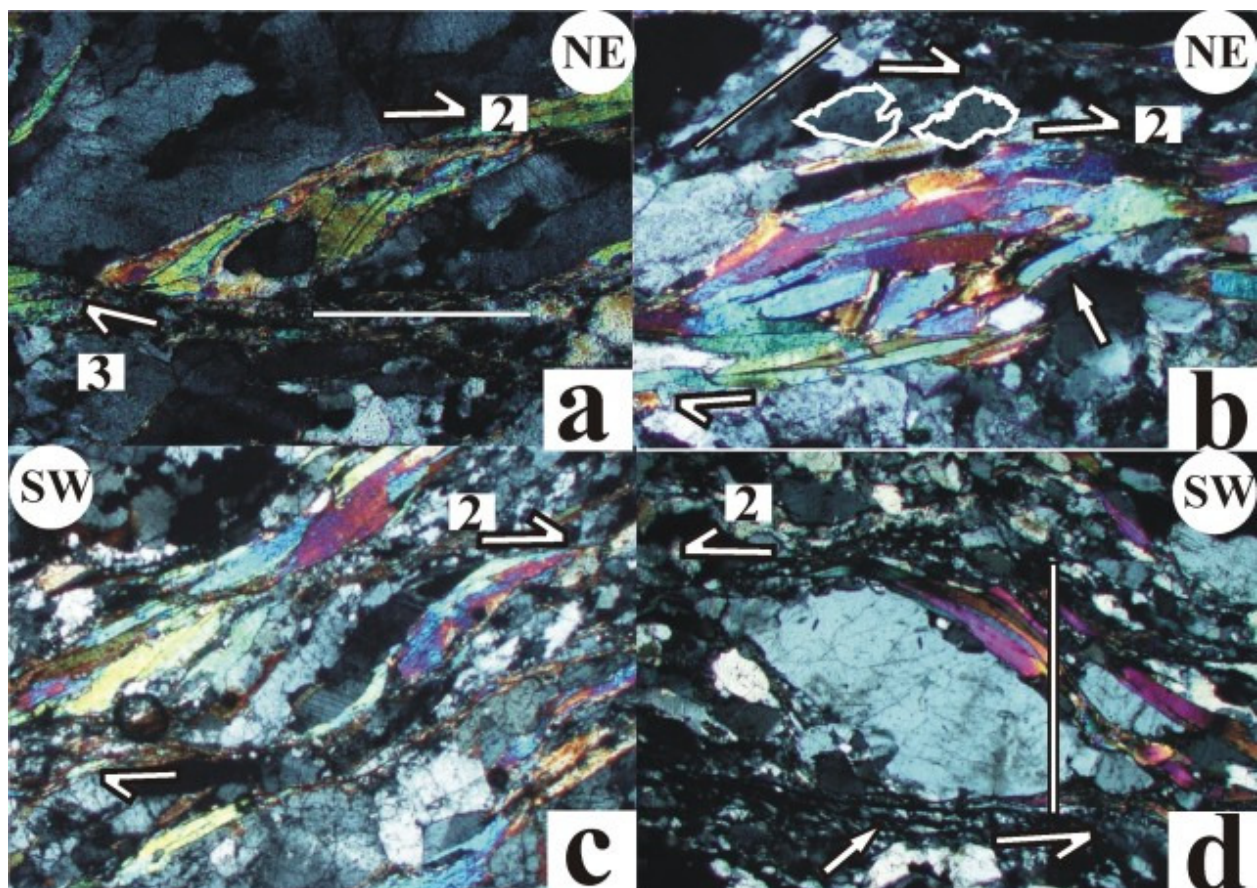
Fis. 3: a. A sigmoid mica fish affected by a top-to-NE (shearing-2) and top-to-NE (down) shear (shearing-3). Strongly swerved cleavages of mica is in sympathy with the shear. The C-plane is traced (white line). (Cross-polarized light; Photo width: 4 mm.). **b.** A composite of bent mica minerals of nearly rectangle shapes and with a haphazard orientation overall defines a lenticle shape and gives a top-to-NE (shearing-2) sense of shearing. (Cross-polarized light; Photo width: 4 mm.). **c.** A stack of mica and quartzo-feldspathic minerals showing a prominent top-to-NE (shearing-2) sense of shearing. (Cross-polarized light; Photo width: 4 mm.). **d.** A weakly sigmoid or a parallelogram shaped alkali feldspar shows a top-to-NE shear (shearing-2). Micas (right hand side) and finer matrix minerals (left hand side) of feldspars were sheared. (Cross-polarized light; Photo width: 4 mm.).
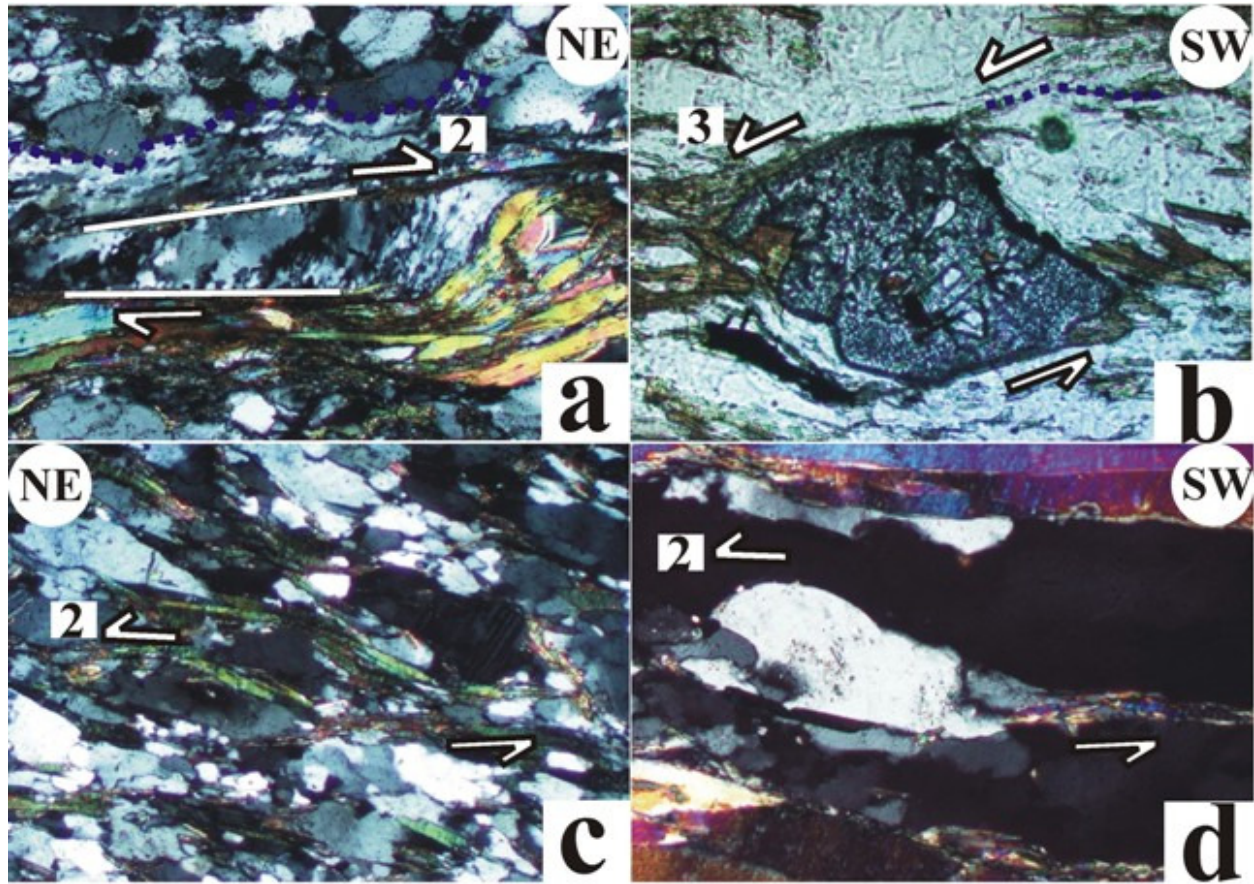
Fig.4: a. Sigmoid matrix define the S fabric: top-to-NE shear (shearing-2). The C-planes are non-parallel (white lines) and are at an angle of 8^0. Below the dashed blue line, quartz took part in shearing. (Cross-polarized light, Photo width: 4 mm.). **b.** A porphyroblastic garnet fish shows a top-to-NE (down) shear sense (shearing-3). Very fine, elongate, discrete biotites also define this shear (dashed blue line). (Plane polarized light; Photo width: 2 mm.). **c.** Discontinuous discrete mica warping larger matrix minerals define a sub-sigmoid/lenticular geometry. A top-to-NE shear ('shearing-2') is displayed. (Cross-polarized light. Photo width: 4 mm.). **d.** A single sigmoid quartz fish with a notch at one of the corners display a top-to-NE shear ('shearing-2'). (Cross-polarized light; Photo width: 2 mm.).
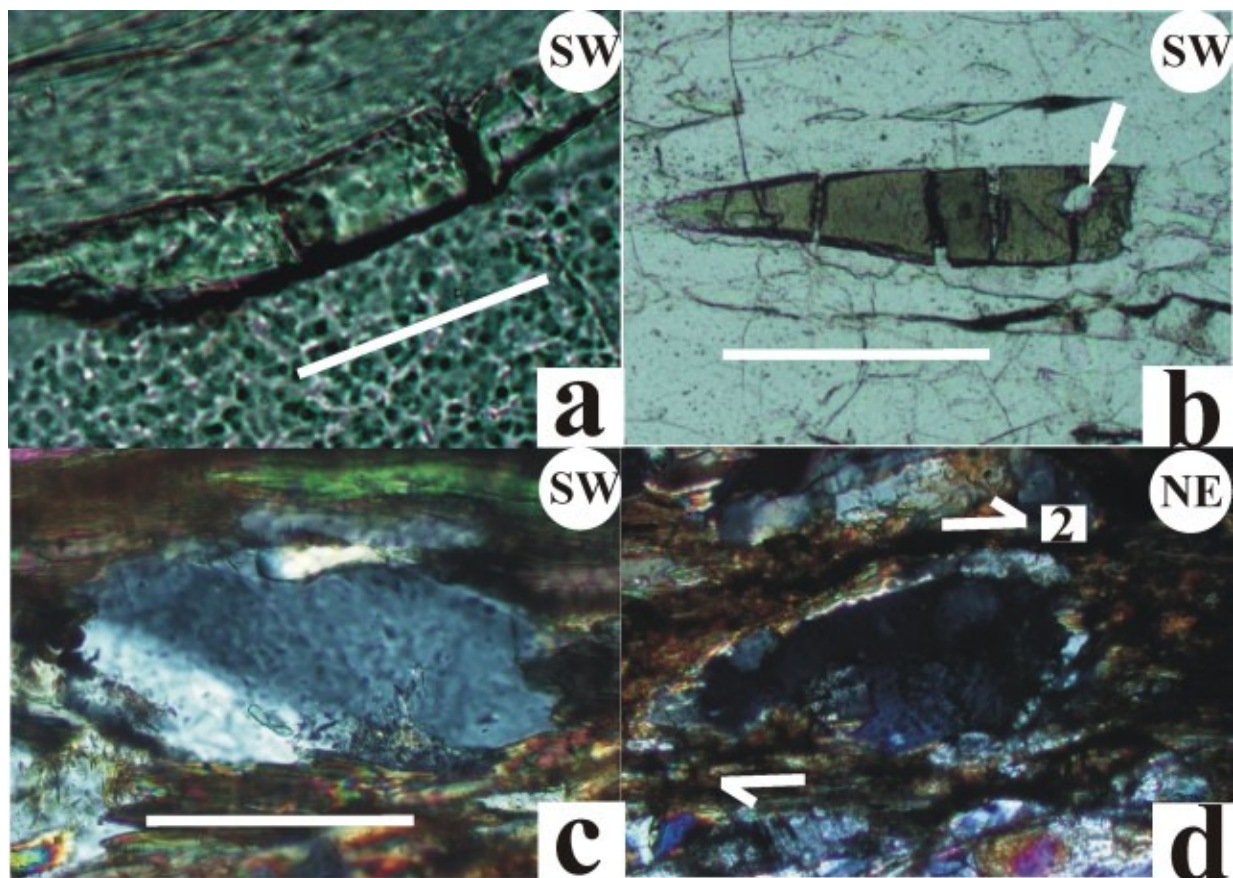
Fig. 5: a. A parallel pull-apart or a boudin of sillimanite grain. A white line shows the orientation of the main foliation deciphered from elsewhere in the thin-section. (Plane polarized light; Photo width: 1 mm.). **b.** A series of pull-apart structures within originally a single tourmaline grain inside quartzo-feldspathic matrix. (Plane polarized light; Photo width: 1 mm.). **c.** A rare spindle-shaped single grain of quartz indicating the tectonic force to be insufficient to completely break apart. (Cross-polarized light; Photo width: 1 mm.). **d.** A rootless intrafolial fold of quartz grain with thick hinge zone and thin unequal limbs dipping towards NE. A relict top-to-SW ('shering-1') is indicated. (Cross-polarized light; Photo width: 1 mm.).
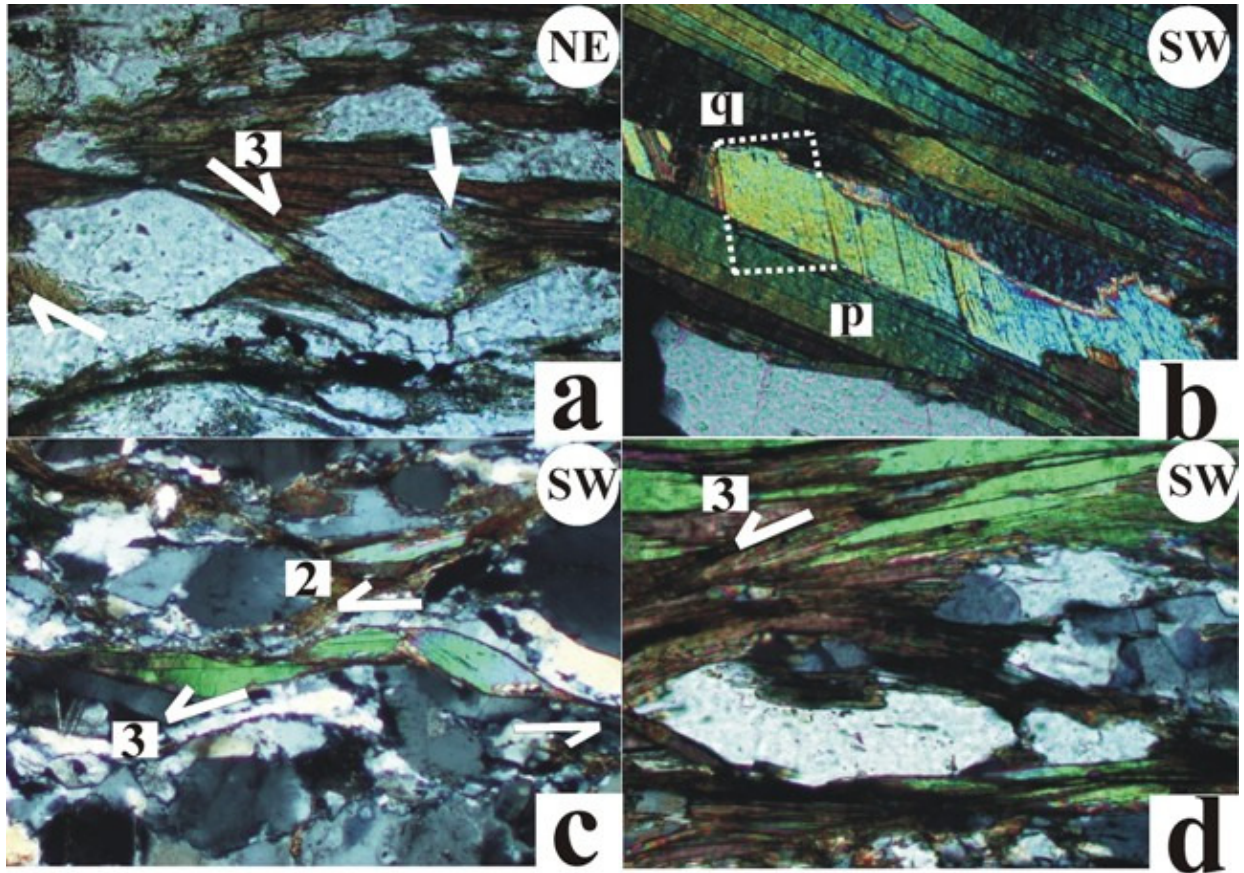
Fig. 6 : a. A pair of single nearly sigmoid quartz fish showing a top-to-NE (down) (shearing-3) sense of shearing. (Plane polarized light; Photo width: 2 mm.). **b.** Bounded by layers of micas, a mica grain assumes a parallelogram shape. (Cross-polarized light; Photo width: 1 mm.). **c.** A single sigmoid-shaped mica fish displays a top-to-NE shear ('shearing-2', white half arrows). Pronounced top-to-NE (down) shear of recrystallized quartz is noted. (Cross-polarized light; Photo width: 2 mm.). **d.** A top-to-NE (down) shear ('shearing-3') has affected foliation micas. (Plane polarized light; Photo width: 2 mm.).
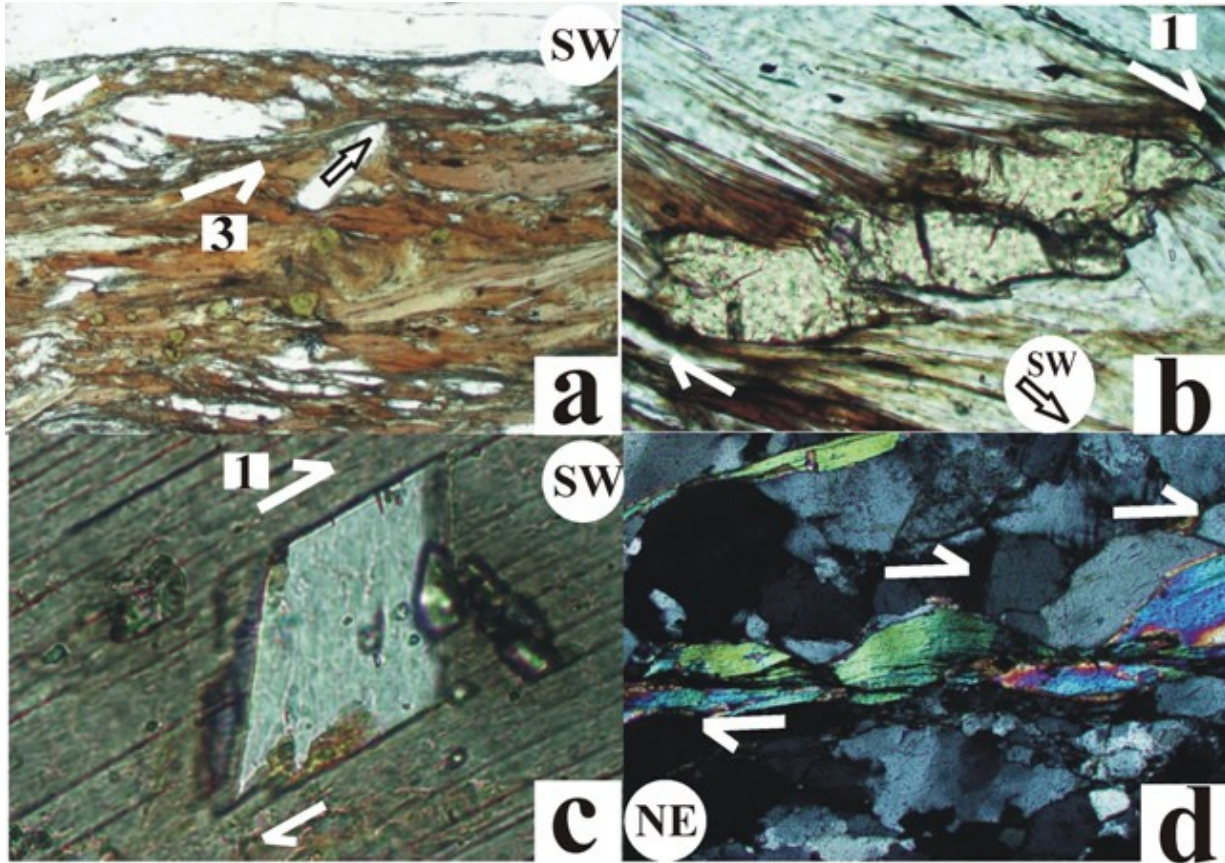
Fig. 7: a. A top-to-NE (down) shear ('shearing-3') is displayed by sigmoid alkali feldspars. A type 2 flanking micro-structure is defined by an elongated grain of alkali feldspar (CE). (Plane polarized light; Photo width: 2 mm.). **b.** A type-1 flanking microstructure defined by nearly sigmoid staurolite as the Host fabric element (HE) and deflected biotites with opposite senses of drag across the HE as the CE. (Plane polarized light; Photo width: 1 mm.). **c.** A parallelogram-shaped muscovite nucleated within a biotite host mineral. The former shows a top-to-SW shear ('shearing-1'). (Plane polarized light; Photo width: 1 mm.). **d.** A top-to-SW brittle shear is displayed by asymmetric duplex of muscovite grain that also defines the foliation plane. (Cross-polarized light; Photo width: 2 mm.).

Flanking Microstructures:

‘Flanking structures’ is deflection of planar or linear fabric elements in a rock alongside a cross-cutting object (Passchier, 2001). Following the same trend, Mukherjee and Koyi (2009) defined flanking microstructures in micro-scales where nucleated minerals defined the cross-cutting elements (CEs) and deflected cleavages and margins of the host grains the host fabric elements (HEs). The former elements cross-cuts the latter planes. The CE minerals that are parallelogram shaped and are inclined to the C-planes indicate ductile shearing and were categorized into the type-1 flanking microstructures. On the other hand, same sense of drag of the CE across the HE minerals indicate preferential growth of the latter and the HE-CE composite together was classified as the type-2 flanking microstructures. Both the type-1 (Fig. 7b-c, 8c, 9c, 10b-c) and the type-2 varieties (Fig. 7a) of these structures were observed in the studied thin-sections. The type-1 structures indicate that the host grain's cleavage planes efficiently acted as ductile C-planes (Fig. 7c). Few of the HE-CE contacts are marked with zones of haziness (Figs. 9b). Inclination and the usual sigmoid and parallelogram shapes of the HE of the type 1 structures indicated a top-to-SW sense of ductile shearing that Mukherjee and Koyi (in press, 1) adjudged to be a 18-16 Ma event. This indicates that the nucleations of those HE minerals were certainly no younger than 16 Ma. The rationale of deciphering the top-to-SW as the earliest deformation in the present micro-structural study is that it is least abundant and occurs as a relict.

Pull-apart structures and boudins:

Pull-apart structures were originally described in micro-scale by Hippereitt (1993) but were latter found also in hand specimen scale by Mukherjee (in press). Singh (1999) provided a comprehensive review on pull-aparts. Mukherjee and Chakraborty (2007) reported the passive folding of foliations inside the opening of the pull-apart minerals in the ZSZ to be of class 3 folds. In the present study, high-grade metamorphic minerals displayed sets of parallel pull-apart (nearly same as boudinage) over a number of parallel zones of breakage (Figs. 5a-b, 11b). Quartz at the V opening is recrystallized (arrow in Fig. 5b). These breakage lines defining the openings are at high angle to the main foliations. At very high magnification, the breakage is found to have taken place along curved planes (Fig. 11b). Further, spindle-shaped isolated boundins of rigid minerals such as quartz are noted. The long axes of the boudins are parallel to the main foliation. These indicate intense brittle-ductile extension parallel to the foliation plane.

Rootless intrafolial folds:

Intrafolial folds of quartz are quite common structures in the ZSZ rocks in micro-scale (Fig. 5d). Their limbs and axial traces dip toward SW, are sub-parallel, and indicate a top-to-NE sense of shearing. The enveloping surfaces of these folds define the ductile shear C-planes of Passchier and Trouw (2005). The fold limbs are unequal in length. Their hinges are rounded and thicker than the limbs. Rootless folds indicate extreme shearing leading to breakage of the limbs from the train of fold.
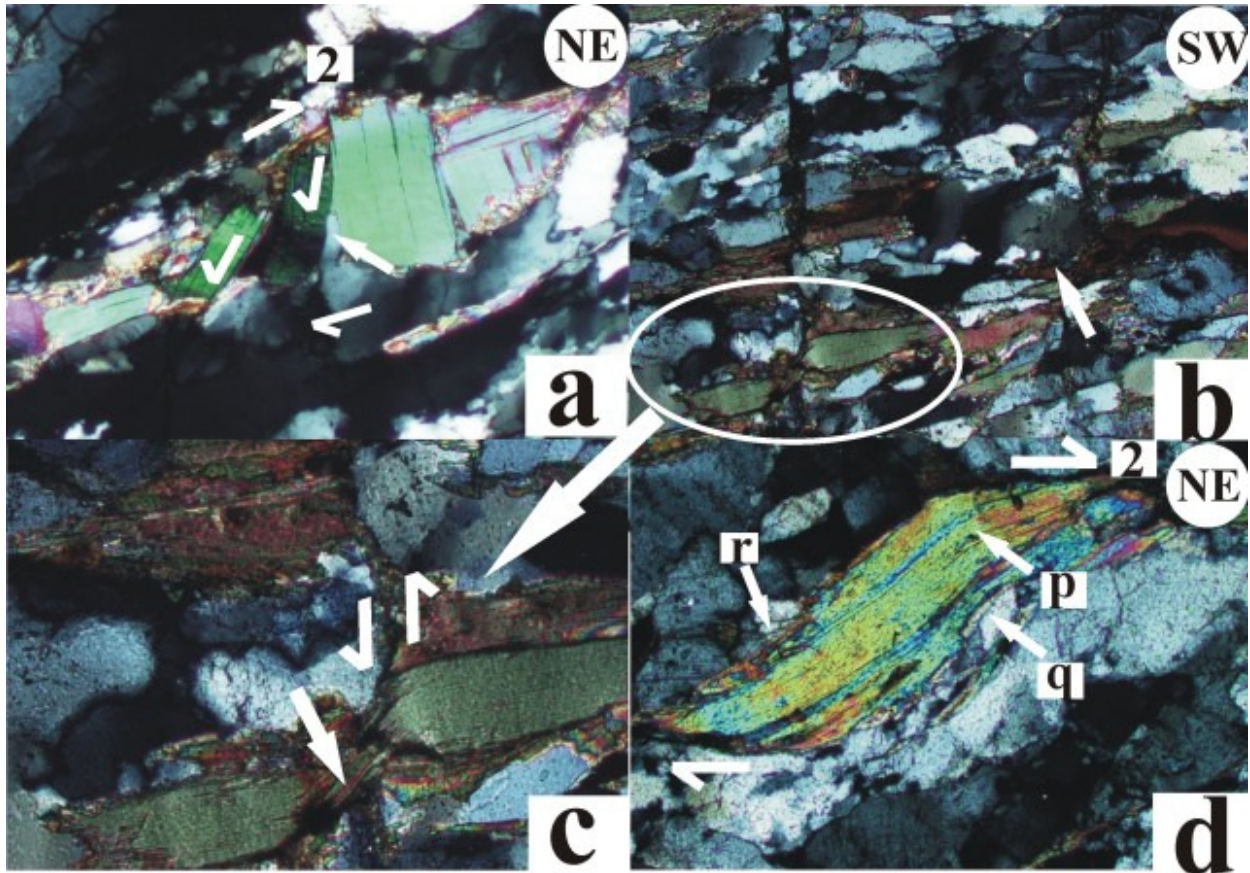
Fig. 8: a. As a response to a top-to-NE shear (shearing-2), muscovites underwent brittle slip along individual boundaries and got rotated. (Cross-polarized light; Photo width: 2 mm.) **b.** Brittle fault at high angle to the foliation plane. A faulted biotite grain at either side of the fault plane act as a marker (ellipse). (Cross-polarized light; Photo width: 0.5 mm.). **c**. Biotite is zoomed and reveals brittle-ductile deformation, normal faulting and an s-type flanking micro-structure. (Cross polarized light; Photo width: 0.5 mm.). **d.** A single sigmoid mica fish. Its crest region (arrow 'p') is kinked. A top-to-NE shear ('shearing-2') is displayed. (Cross polarized light; Photo width: 1 mm.).
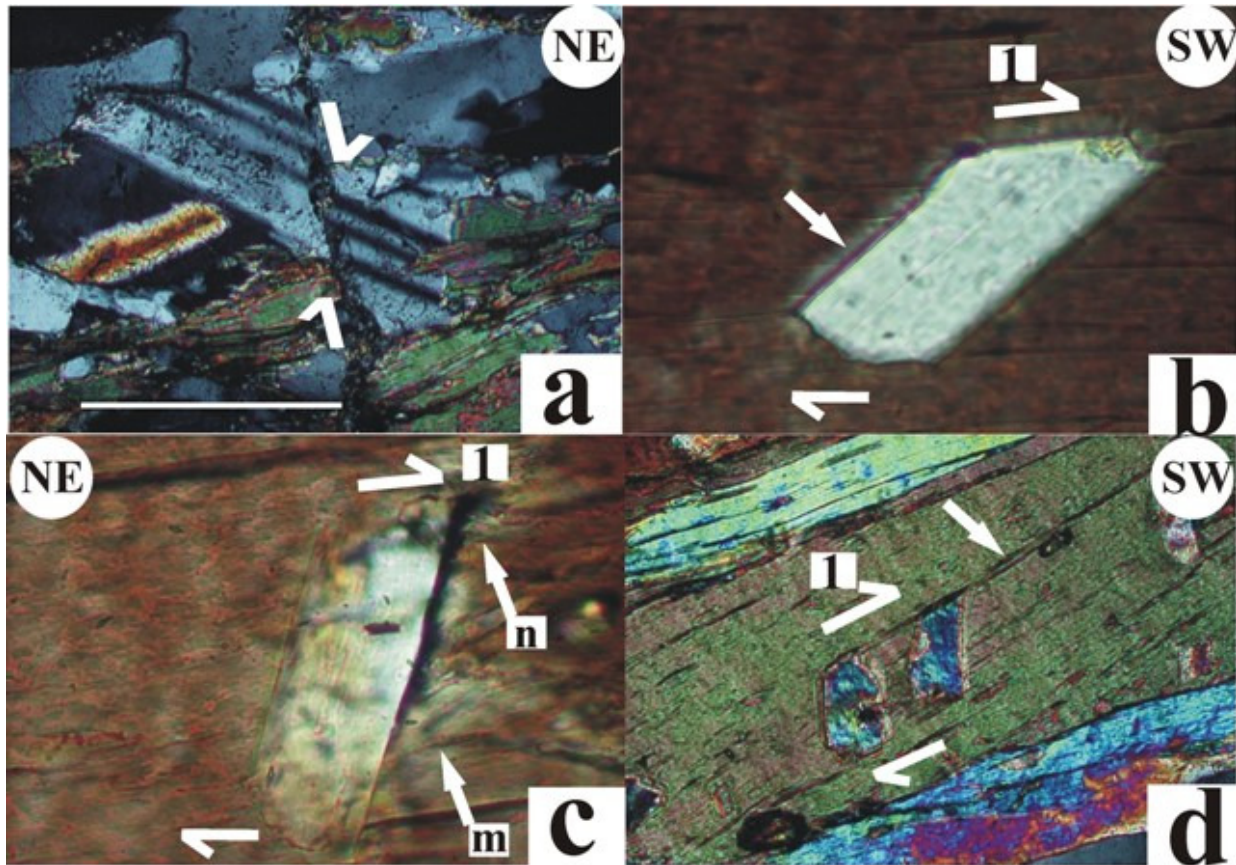
Fig. 9: a. A brittle normal fault in micro-scale (Cross-polarized light; Photo width: 0.5 mm.). **b.** A nearly parallelogram-shaped muscovite grain nucleated inside a biotite host mineral. The shape of the nucleated mineral indicates a top-to-SW shear ('shearing-1'). (Plane polarized light; Photo width: 0.5 mm.). **c.** A nearly parallelogram-shaped muscovite grain nucleated inside a biotite host mineral. Top-to-SW sense sheared ('shearing-1'). (Plane polarized light; Photo width: 0.5 mm.). **d.** A pair of adjacent nearly parallelogram-shaped muscovite grain nucleated inside biotite host mineral. Top-to-SW sheared ('shearing-1'). (Cross polarized light; Photo width: 1 mm.).
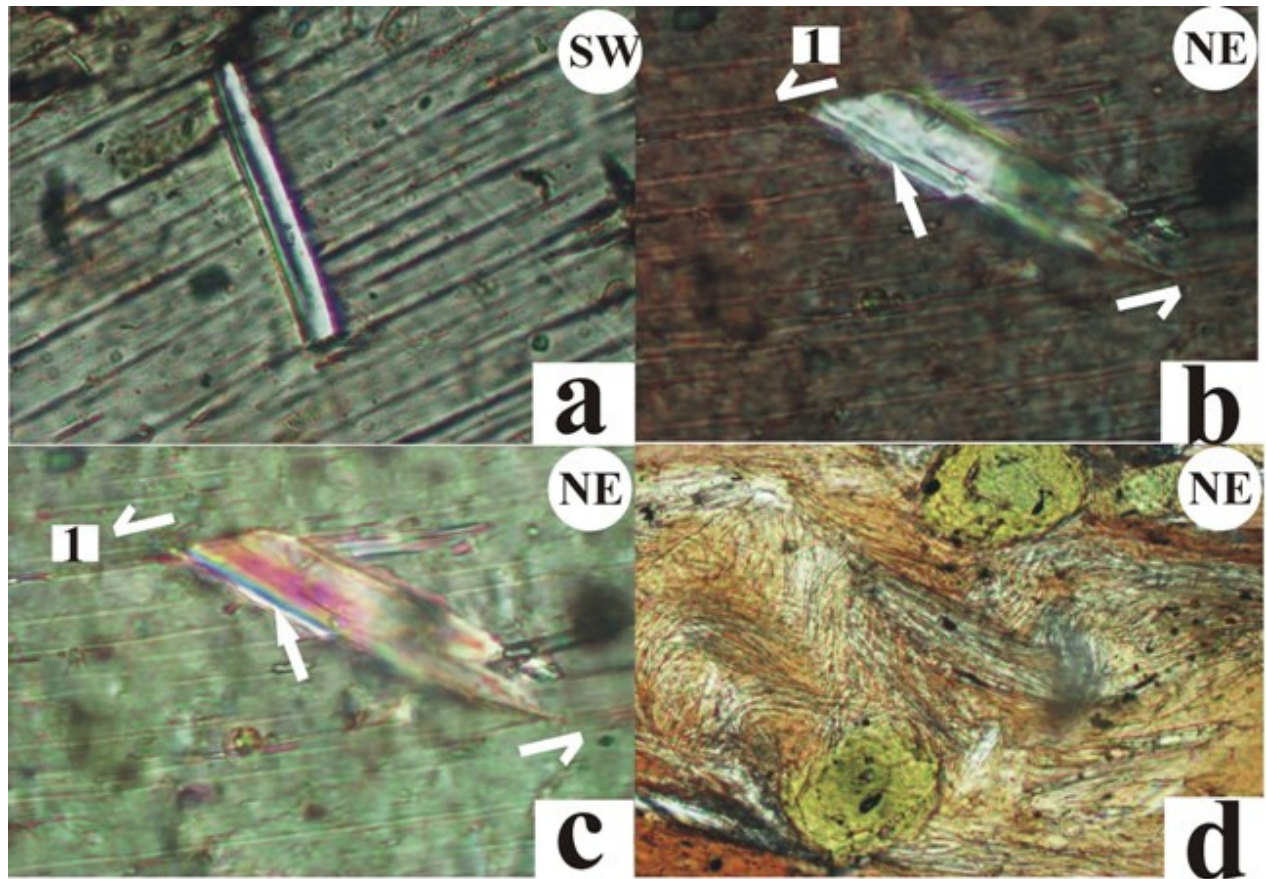
Fig. 10: a. An elongated unsheared muscovite grain nucleated within another muscovite grain. (Plane polarized light; Photo width: 1 mm.). **b & c:** A nearly parallelogram-shaped muscovite grain nucleated inside biotite host mineral. The shape of the nucleated mineral indicates a top-to-SW shear ('shearing-1'). (Plane and cross polarized lights, respectively; Photo width: 0.5 mm.). **d.** Kinked aggregate of biotites and sillimanites that define the main foliation. (Plane polarized light; Photo width: 1 mm.).
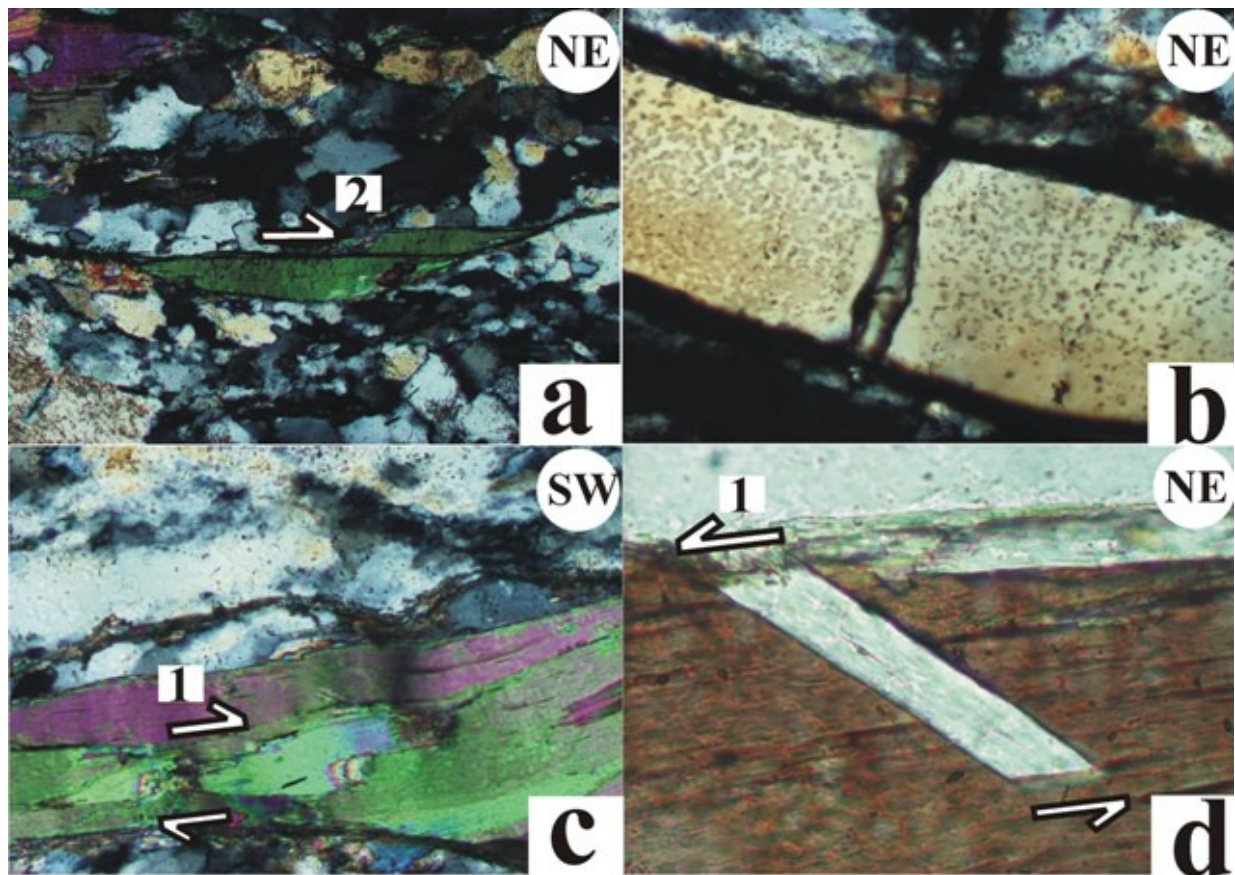
Fig. 11: a. Sharp slip of a single muscovite grain along a brittle fault plane to a top-to-NE sense. (Cross-polarized light; Photo width: 1 mm.). **b.** Zoomed photo of parallel pull-apart reveals that the opening is actually curved. (Cross polarized light; Photo width: 0.5 mm.). **c.** Inside a muscovite host mineral, two nucleated muscovite grains of unequal sizes underwent a top-to-SW shear ('shearing-1') giving rise to their asymmetric shapes and notches (mouths).(Cross-polarized light; Photo width: 1 mm.). **d.** A parallelogram-shaped muscovite nucleated within a biotite host mineral. A top-to-SW shear ('shearing-1') is displayed by muscovite grain. (Plane polarized light; Photo width: 0.5 mm.).
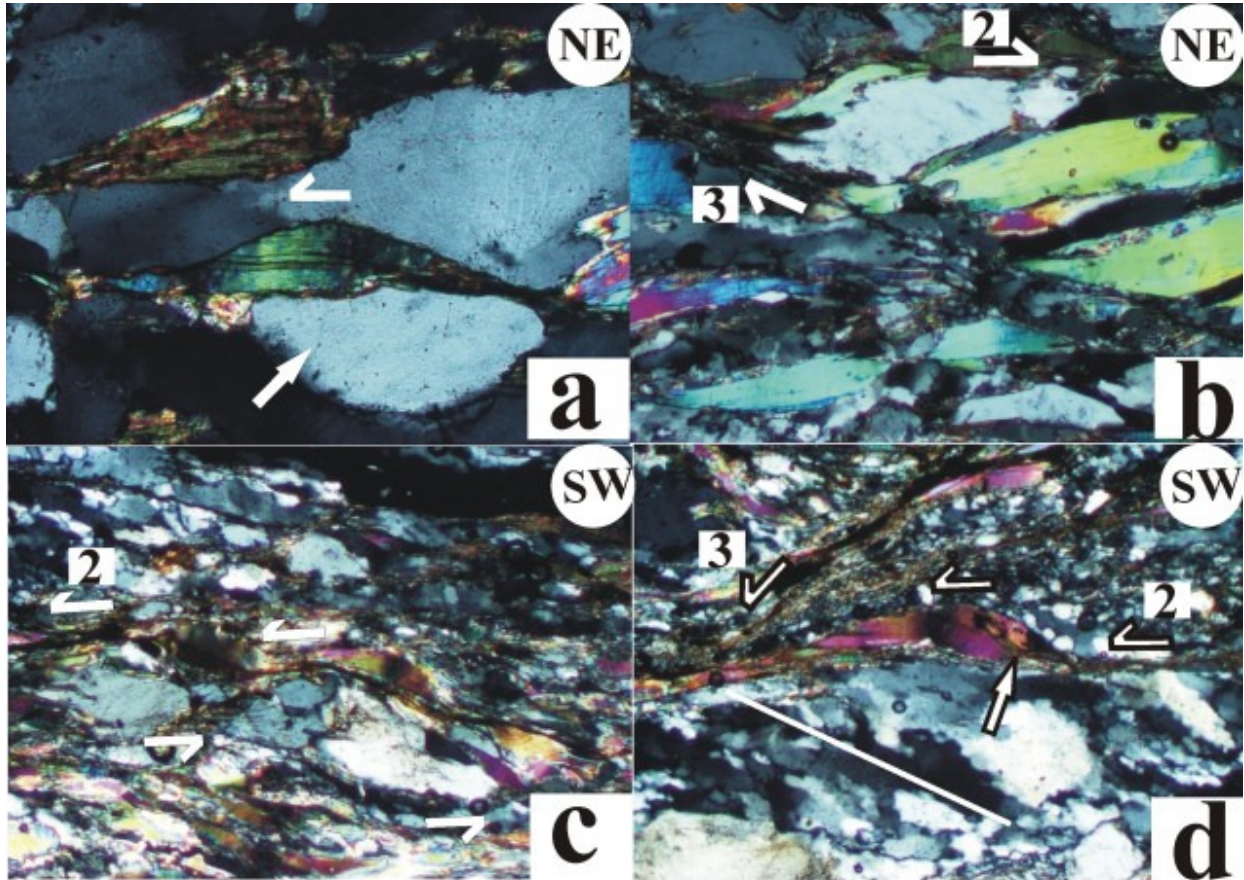
Fig. 12: a. A top-to-SW shear is indicated by a muscovite grain that overrode another grain of muscovite. The brittle fault plane sharply cuts an otherwise rounded grain of a rigid grain of quartz (arrow) (Cross-polarized light; Photo width: 1 mm.). **b.** Top-to-NE (down) ('shearing-3') and a top-to-NE shear ('shearing-2') are deciphered from sigmoid-shaped single larger muscovites and alkali feldspar. (Cross-polarized light; Photo width: 1 mm.). **c.** A top-to-NE shear (shearing-2) is indicated by an aggregate of quartzo-feldspathic minerals (Cross-polarized light. Photo width: 1 mm.). **d.** A top-to-NE (down) shear (shearing-3) is indicated by an aggregate of fine-grained quartzo-feldspathic minerals. A top-to-NE shear ('shearing-2') is deciphered from recrystallized and oriented (white line) quartz in the bottom half of the photo (Cross-polarized light, Photo width: 1 mm.).

Other micro-structures:

A top-to-SW sense of brittle shearing along Y-planes is indicated by asymmetric nearly trapezoid-shaped minerals- most commonly micas (Figs. 7d, 12a). These trapezoids define the P-planes (as per the terminology of Passchier and Trouw, 2005). Mukherjee (2007) and Mukherjee and Koyi (in press 1, in press 2) previously recognized such shapes of grains as characteristic of brittle shear sense from a number of shear zones in the Himalaya. In some cases the brittle plane sharply cut across rigid minerals in the matrix (Fig. 12a). The brittle shear plane dips towards NE and is parallel to the ductile shear C-plane. In few cases, minerals are sharply faulted across it without any decipherable dragging (*e.g.* Fig. 9a). In one example, imperfect book-shelf gliding of muscovite grains indicates inter-granular slip under an overall top-to-NE sense of shearing (Fig. 8a). Northeasterly dipping sharp normal faults cut across the pre-existing ductile shear planes (Fig. 8b-c, 9a). At high magnification, individual biotite grain margins as well as their cleavage planes were found to be brittle-ductilely affected by these fault planes (Figs. 8c). On the other hand, more competent minerals such as plagioclase feldspar underwent sharp slip without any drag effect. Fault gouge is expected in such deformation (Passchier and Trouw, 2005) but were not encountered in the studied thin-sections. In the present micro-structural study, micas are found to be most vulnerable to deformation presumably because of their lower competence. Nearly straight limb but round hinged folds of dense intergrowth of biotite and sillimanite was noted within the foliation plane (Fig. 10d) but whether these belong to the pre-Himalayan D_1 or late phase D_3 folds (as per the compilation by Mukherjee and Koyi in press, 1) remained indeterminate.

Conclusions

Micro-structural study of the rocks of the Zanskar Shear Zone revealed an oldest top-to-SW shearing of ~22-16 Ma; and subsequent top-to-NE sense of shearing and finally a top-to-NE (down) sense of ductile shearing of ~18-16 Ma. The effect of combined simple shear and channel flow mode of deformation and extrusion are well manifested by micas that act as the commonest shear sense indicators. The shape asymmetries as well as the cleavage plane orientation with respect to the C-planes of mineral fish act as reliable shear sense indicators. Few fish are affected by shearing of different phases. Specific orientation of fish indicates they are produced dominantly by either a top-to-SW or a –NE simple shear. The top-to-SW sense of shear is also well demonstrated by the type-1 flanking microstructures defined by sheared nucleated minerals as the cross-cutting elements and cleavages and grain boundaries of host minerals as the host fabric elements. Rigid minerals are boudinaged by pronounced pulling along the main foliation. Rather frequent (rootless) intrafolial folds with axial planes dipping towards southwest indicate a top-to-NE sense of shearing. A top-to-SW brittle shear sense is displayed by asymmetric trapezoid-shaped duplexes of micas. The brittle Y-planes, which are parallel to the preexisting ductile C-planes, at places are so pervasive that they cut rigid minerals. Amongst all the minerals, micas are most vulnerable to ductile and brittle deformations. Rare micro-structures that are possibly not of any regional significance are (i) intense folding of sillimanite-biotite woven foliations, and (ii) haphazard growth of minerals that overall define the main foliations.

References

Beaumont, C., Jamieson, R.A., Nguyen M.H. and Lee, B. (2001) Himalayan tectonics explained by extrusion of a low-viscosity crustal channel coupled to focused surface denudation. Nature, v. 414, pp. 738-742.

Bell, T.H. and Cuff, C. (1989) Dissolution, solution transfer, diffusion versus fluid flow and volume loss during deformation/metamorphism. J. Meta. Geol. v. 7, pp. 425-447.

Bèrthe, D., Choukroune, P. and Jegouzo, P. (1979) Orthogneiss, mylonite and non-coaxial deformation of granite: the example of the south Armorican shear zone. J. Struct. Geol., v. 1, pp. 31-42.

Dèzes, P.J. (1999) Tectonic and Metamorphic evolution of the central Himalayan domain in southeast Zanskar (Kashmir, India). Ph.D. Thesis. University of Lausanne, Switzerland. 160p.

Dèzes, P.J., Vannay, J.C., Steck, A., Bussy, F. and Cosca, M. (1999) Synorogenic extension: Quantitative constraints on the age and displacement of the Zanskar shear zone. Geol. Soc. Am. Bull., v. 111, pp. 364-374.

Godin, L., Grujic, D., Law, R.D. and Searle, M.P. (2006) Channel flow, extrusion and exhumation in continental collision zones: an introduction. In: *R.D. Law and M.P. Searle (eds.)* Channel flow, extrusion and exhumation in continental collision zones. Geol. Soc. London, Spec. Pub., v. 268, pp. 1–23.

Herren, E. (1987) Zanskar Shear Zone: northeast southwest extension within the Higher Himalaya (Ladakh, India). Geology, v. 15, pp. 409-413.

Hippertt, J.F.M. (1993) 'V' pull-apart microstructures: a new shear sense indicator. J. Struct. Geol, v. 15, 1394–403.

Lister, G.S., and Snoke, A.W. (1984) S-C Mylonites. Journal Struct. Geol, v. 6, pp. 617-638.

Mukherjee, S. (2005) Channel flow, ductile extrusion and exhumation of lower-middle crust in continental collision zones. Current Sci, v. 89, pp. 435–436.

Mukherjee, S. (2007) Geodynamics, deformation and mathematical analysis of metamorphic belts of the NW Himalaya. Unpublished Ph.D. thesis. Indian Institute of Technology Roorkee. 267 p.

Mukherjee, S. (in press) Macroscopic 'V' pull-apart structure in garnet. Photo of the Month. J. Struct. Geol.

Mukherjee, S. and Chakraborty, R. (2007) Pull-apart micro-structures and associated passive folds. In: *J. Aho (ed.)* Annual Transactions of the Nordic Rheology Society v. 15, pp. 247-252. 16th Nordic Rheology Conference, Stavanger, Norway.

Mukherjee, S. and Koyi, H. A. (2009) Flanking Microstructures. Geol. Mag, v. 146, pp. 517-526.

Mukherjee, S. and Koyi, H.A. (in press, 1) Higher Himalayan Shear Zone, Zanskar Section-Microstructural Studies and Extrusion Mechanism by a Combination of Simple Shear & Channel Flow. Int. Journal Earth Sci., online published, doi: 10.1007/s00531-009-0447-z.

Mukherjee, S. and Koyi, H.A. (in press, 2). Higher Himalayan Shear Zone, Sutlej section: structural geology and extrusion mechanism by various combinations of simple shear, pure shear and channel flow in shifting modes. Int. Journal Earth Sci., online published, doi: 10.1007/s00531-009-0459-8.

Mukherjee, S. and Pal, P. (2000) Tectonic structures of the Karakoram metamorphic belt, its significance in the Geodynamic Evolution. Unpublished Report. Summer Undergraduate Research Award. University of Roorkee.

Passchier, C.W. and Trouw, R.A.J. (2005) Microtectonics. Springer Verlag, Heidelberg. p.p. 1-366.

Patel, R.C., Singh, S., Asokan, A., Manickavasagam, R.M. and Jain, A.K. (1993) Extensional tectonics in the Himalayan orogen, Zanskar, NW India. In: *P.J. Treloar, M.P. Searle (eds.)* Himalayan Tectonics, Geol. Soc. Lond. Spec. Publ., v. 74, pp. 445-459.

Searle, M.P., Cooper, D.J.W. and Rex, A.J. (1988) Collision tectonics of the Ladakh-Zanskar Himalaya. In: *R.M. Shackleton, J.F. Dewey and B.F. Windley (eds.)* Tectonic evolution of the Himalayas and Tibet. Philosophical Transaction of the Royal Society, London, v. A326, pp 117–150.

Singh, K. (1999) Pull apart microstructures in feldspar from Chail Thrust Zone, Dhauladhar Range, Western Himachal Pradesh. In: *A. K. Jain and R.M. Manickavasagam (eds)*. Geodynamics of the NW Himalaya. Gondwana Research Group Memoir, v. 6; pp. 117–23. Osaka.

Steck, A., Spring, L., Vannay, J.C., Masson, H., Stutz, E., Bucher, H., Marchant, R., and Tièche, J.C., (1993) Geological transect across the Northwestern Himalaya in eastern Ladakh and Lahul (A model for the continental collision of India and Asia): Eclo. Geol. Helv, v. 86, p. 219.

Treagus, S.H. and Lan, L. (2000) Pure shear deformation of square objects, and applications to geological strain analysis. J. Struct. Geol, v. 22, pp. 105-122.

Walker, J. D., Martin, M. W., Bowring, S. A., Searle, M. P., Waters, D. J. and Hodges, K. V. (1999) Metamorphism, melting and extension: age constraints from the High Himalayan slab of southeast Zanskar and northwest Lahul. Geol., v. 107, pp. 473-495.

Walker, J. D., Searle, M. P. and Waters, D. J., 2001. An integrated tectonothermal model for the evolution of the Higher Himalaya in western Zanskar with constraints from thermobarometry and metamorphic modeling. Tectonics, v. 20, 810-833.

Yin, A. (2006) Cenozoic tectonic evolution of the Himalayan orogen as constrained by along-strike variation of structural geometry, extrusion history, and foreland sedimentation. Earth Sci. Rev., v. 76, pp. 1-131.

About the author

Dr. Soumyajit Mukherjee is Senior Lecturer, Department of Earth Sciences, Indian Institute of Technology Bombay, Mumbai. He received his Ph.D. (2007) and M.Tech. in Applied Geology (2002) from IIT, Roorkee. His areas of research are structural geology, tectonics and Himalayan geology. Recipient of several national awards, Dr. Mukerjee also received 'Hutchison Young Scientist Award' from the IUGS in 2004. He also worked in the Hans Ramberg Tectonic Lab., Uppsala University as a 'Guest Researcher' during 2005-2006.